Ising and Bloch walls of phase domains in two-dimensional parametric wave mixing

Ye. Larionova,[1,*] U. Peschel,[2] A. Esteban-Martin,[3] J. Garcia Monreal,[3] and C. O. Weiss[1]
[1]*Physikalisch-Technische Bundesanstalt, 38116 Braunschweig, Germany*
[2]*Institut für Festkörpertheorie und Theoretische Optik, Friedrich-Schiller Universität, Jena, D-07743, Germany*
[3]*Departament D'Òptica, Universitat de València, València, Spain*
(Received 20 June 2003; revised manuscript received 20 October 2003; published 3 March 2004)

Oscillators driven by a degenerate wave mixing process are bistable in the phase of the generated radiation. In systems with a large Fresnel number, domains of opposite phase form therefore spontaneously. A simple model predicts a real field in which phase domains are separated by Ising-type walls. In this paper we show experimentally (using complex field reconstruction from measurements) and theoretically (by an extended model) that the optical field can be real as well as complex valued and that complex field fronts are related to the front curvature.

DOI: 10.1103/PhysRevA.69.033803 PACS number(s): 42.65.Sf, 42.65.Hw, 42.65.Pc

I. INTRODUCTION

Systems close to a symmetry breaking bifurcation are often describable by a real-valued order-parameter equation as, e.g., the Swift-Hohenberg equation (SHE) [1]. We found in Ref. [2] that such a description is qualitatively adequate for pattern formation in a degenerate four-wave mixing resonator. In this article we show that such approximation is insufficient, if one leaves the bifurcation point. We investigate here degenerate four-wave mixing in a photorefractive crystal ($BaTiO_3$) in a cavity. Above the emission threshold light has two possible phase values with respect to the pump field phase, differing by π, thus the field is a real variable [1]. As a consequence, domains of opposite phase coexist in systems with a large Fresnel number. In case of real-valued fields as described by the SHE [1] one would expect these phase domains to be separated by "black" domain walls, across which the amplitude of the field crosses zero ("Ising walls" [3]).

A closer inspection of the experimentally generated fields, however, showed that the SHE approximation is insufficient. The fronts separating phase domains are not always black (i.e., the field goes through zero) but are often "gray" (Fig. 1). Hence, the field connects the two opposite phase values along a path in the complex plane without touching the zero point ("Bloch wall") and, generally speaking, an asymmetry has developed. Asymmetric domain walls can form for two reasons. First a spontaneous symmetry breaking can occur already in the respective one-dimensional system. A transition from a symmetric so-called Ising to an asymmetric Bloch wall occurs [3,4]. The second reason, which we investigate in more detail, is a typical two-dimensional (2D) effect. A basically one-dimensional wall, which exists in a two-dimensional environment, can have a curvature. This also breaks the symmetry with the consequence of a complex field (Bloch) wall. Both cases have two things in common. First the asymmetry restricts the validity of real-valued models. Hence, phase structures, more complex than the steplike phase profiles of the real-valued case, are possible. Second, in almost every case a loss of symmetry breaks the internal balance of forces. Consequently a motion occurs. In this paper we show both experimentally and on the basis of a numerical model that real as well as complex fronts occur and we investigate the relation between curvature and complex nature of domain fronts.

We study the structure of the fronts experimentally observed, on the one hand, by fitting the front profiles by analytic front expressions. On the other hand, to measure the front structures in 2D we use a technique permitting to reconstruct the full 2D complex field from the experiment. It uses a reference field for spatial heterodyning in recording the emitted field, and a Fourier technique for extracting the complex field from the recorded interferograms. This permits to study the 2D fronts in detail.

In addition a more complete model than the real SHE approximation is used to study the fronts of phase domains, providing qualitative agreement with the experimental observations.

II. EXPERIMENT

The experimental arrangement is the same as used in Ref. [2]. It uses a $BaTiO_3$-crystal inside a linear resonator. The

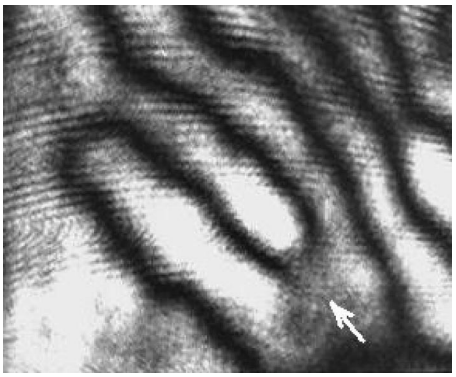

FIG. 1. Domain boundaries showing black and gray (arrow) fronts in the intensity picture obtained in four-wave mixing in a $BaTiO_3$ resonator.

*Email address: yevgeniya.larionova@ptb.de

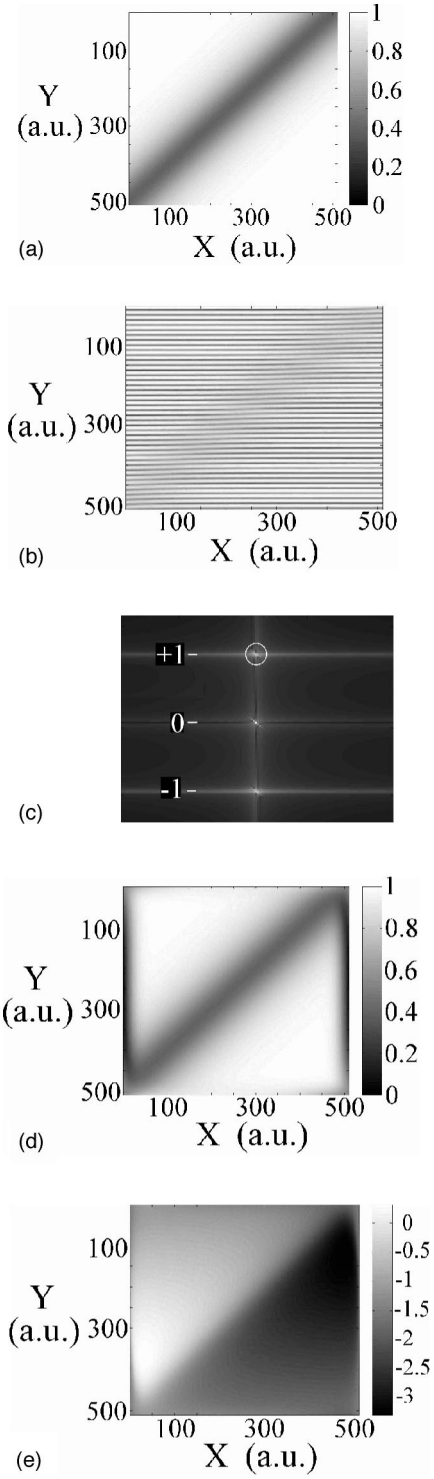

FIG. 2. Illustration of the reconstruction of the complex optical field by the Fourier technique. (a) Original intensity picture with 40% of grayness [amplitude minimum is 40% of maximum amplitude (white)], (b) interferogram, obtained by the interference with an inclined plane wave (reference field), (c) Fourier spectrum with zero and ±1 diffraction orders (the distance between the orders and the width of orders correspond to the spatial frequency offset and spatial details of the field, respectively); the white circle shows the width of the Gaussian filter used, (d) and (e) reconstructed amplitude and phase of the complex field. *X*, *Y* are the transverse spatial coordinates in a.u.

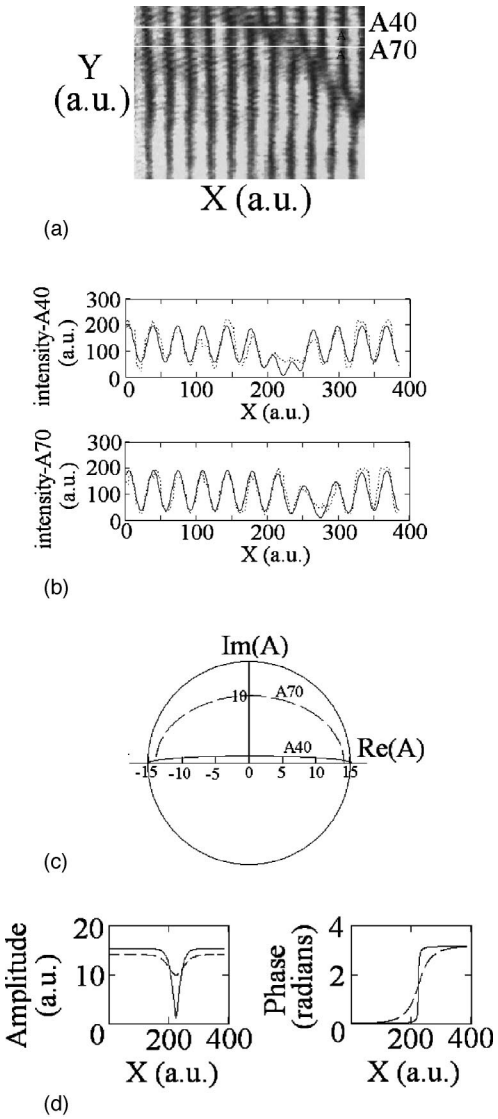

FIG. 3. (a) Experimental interferogram of a domain front, (b) fit of cuts A70 and A40 of the experimental interferogram with analytical front solution of Ref. [3]; solid lines: fit, dotted lines: experimental data, (c) corresponding plots of complex field across the fronts, indicating that A70 is a complex front and A40 is very close to a real front, units correspond to (d), (d) reconstructed phase and amplitude of field for two cuts across the front, solid lines: cut A40, dashed lines: cut A70. The near zero amplitude minimum of A40 and its steplike phase profile identify A40 as a (near) Ising front. The shallow amplitude minimum and the smooth phase profile identify A70 as a complex, Bloch front.

crystal is pumped by two opposed pump waves from a single frequency 514 nm Ar^+ laser. The generated waves propagate in the same linear resonator, which forces them to be degenerate. To allow arbitrary field patterns to be resonant, the resonator is of "self-imaging" type [5], which means that the diffraction is precisely compensated by lenses. In such a resonator all transverse modes have equal frequencies and, correspondingly, any field pattern can be resonant. We avoid in general the exact compensation of diffraction by the lenses because in this case the unknown and uncontrolled aberrations of the lenses become dominant. Thus we use a residual

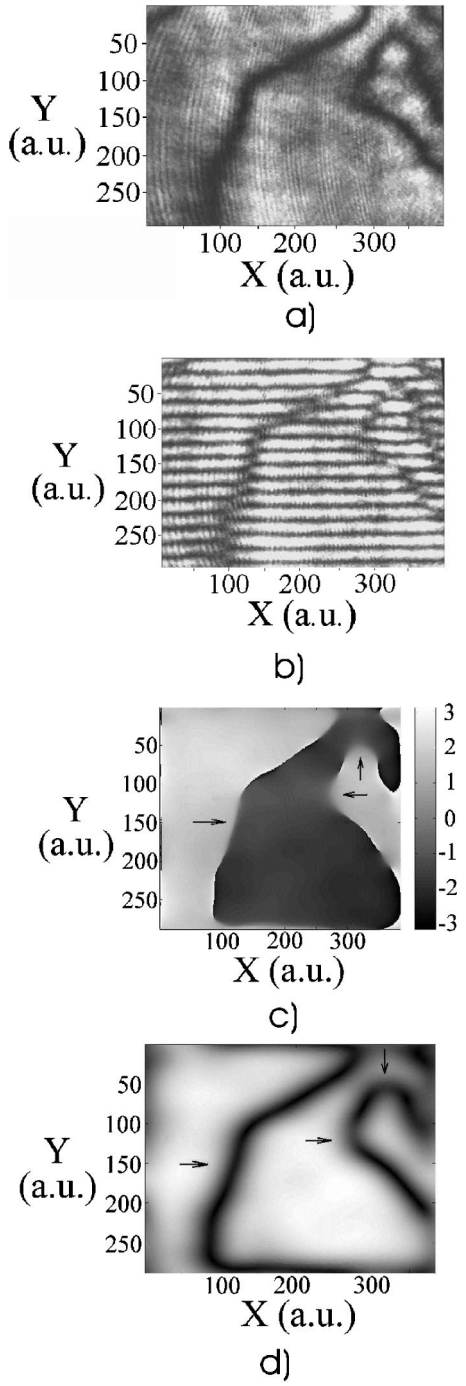

FIG. 4. Experimental intensity picture (a) and its interferogram (b), showing that adjacent domains have opposite phase; 2D-phase (c) and -amplitude (d) of four-wave mixing field reconstructed by the Fourier method from (b) (X, Y are the transverse spatial coordinates). Gray front pieces are marked by arrows (for the unphysical phase changes of 2π across certain front pieces see explanation in text).

uncompensated diffraction to smooth out the aberrations. The effect is a reduction of Fresnel number, which, however, can still be as large as 10^4 so that patterns with fine structural details are possible. The tuning of the resonator on a wavelength scale is done by piezo elements and the control technique for the detuning is described in Ref. [6].

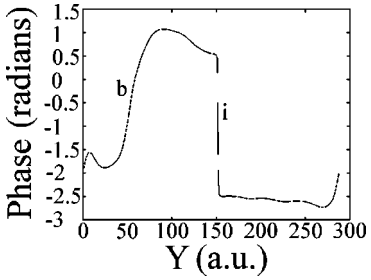

FIG. 5. Phase as a function of Y at $X=315$ of reconstructed phase picture Fig. 4(c) (b: complex front, i: real front).

The crystal is directly imaged into a CCD camera so that near field intensity images are recorded. To record the complex field, phase information must be obtained through interference. We use a reference wave (split from the pump laser beam) at a certain angle to the generated field. The angle defines the spatial frequency offset which has to be larger than the width of the Fourier spectrum of the field in order to reconstruct the spatial details of the complex field.

The technique is analogous, on the one hand, to the reconstruction of a complex field in holography. Figure 2 illustrates the technique by a numerical example. Figure 2(a) shows the intensity of a "gray" front. Figure 2(b) shows the interferogram. The Fourier transform [Fig. 2(c)] of the interferogram Fig. 2(b) contains the zero-order component and the ±1 diffraction orders. The zero-order component is the intensity fluctuation spectrum and contains no phase information.

The ±1 diffraction orders both contain the full information about the complex field. The complex field is therefore retrieved by cutting away all except one of the diffraction orders [as shown in Fig. 2(c) by a white circle around the +1 diffraction order]. The complex field in the object plane is reconstructed by inverse Fourier transformation. Figures 2(d) and 2(e) show the reconstructed amplitude and phase distribution of the complex field corresponding to the intensity picture [Fig. 2(a)] and the interferogram [Fig. 2(b)].

For the filter [Fig. 2(c)] which passes the selected diffraction component a Gaussian profile is used. Its width is chosen to pass most of the information of the diffraction order and at the same time to suppress the zero-order component and the negative diffraction order as much as possible. This filtering requires a separation of diffraction orders larger than

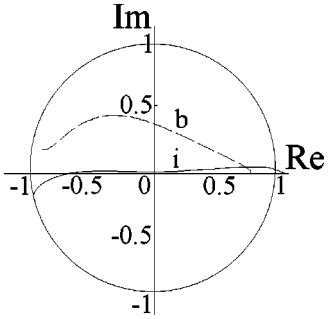

FIG. 6. Complex field plot across front for real (i) and complex (b) pieces of the cut Fig. 5.

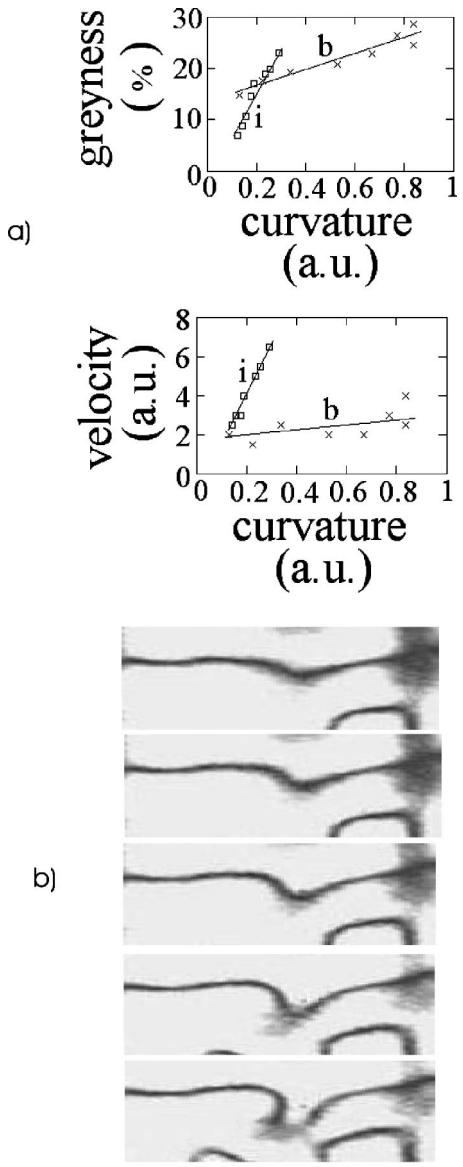

FIG. 7. (a) Plots of front grayness vs a rough measured front curvature and of front velocity vs front curvature, constructed for two fronts taking arbitrary from the experimental recording. (b) Recordings of one of fronts straightening in time. Time between pictures is 2 s. The succession of pictures shows that the front becomes darker as it becomes less curved.

the width of the diffraction orders. In other words, it requires a large enough angle with the reference field. [It may be mentioned that this spatial reconstruction of the complex field is completely analogous to the technique used in Ref. [7] to reconstruct the temporal evolution of the complex field by "temporal" heterodyning. The frequency offset used there for the reference wave corresponds here, in the space domain, to the angle between generated field and reference wave ("spatial frequency offset")].

Another method to retrieve the phase and amplitude changes across a front is by fitting an experimental interferogram with a simple complex valued expression as

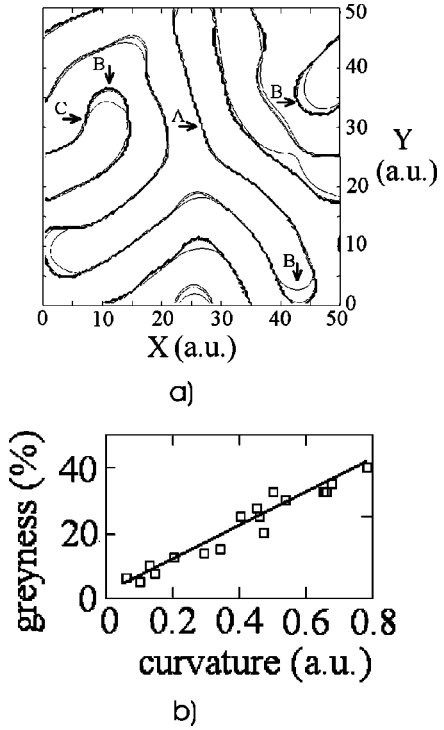

FIG. 8. (a) Phase structure of moving pattern (detuning=0.2), *A* is a real front, *B* is a complex front, *C* is a transition point between real and complex front, (b) grayness vs curvature of fronts constructed from phase pictures such as (a) [compare with Fig. 7(b)], the relation of phase and amplitude profile was assumed to obey Eq. (1).

$$A(X) = \sqrt{P_1}\tanh\left(\frac{X - X_0}{W}\right) \pm i\frac{\sqrt{P_2}}{\cosh\left(\frac{X - X_0}{W}\right)}. \qquad (1)$$

In 1D, such a formula is known for the Bloch-front and its Ising-limit [3] and it is likely that it can also approximate a curved structure. P_1 is the power of the plane-wave state, P_2 accounts for the amount of grayness of the front. X_0 is the position of the front and W is its width.

Figure 3 shows such fits to an experimental interferogram [see Fig. 3(a)]. A phase change of π across the front is evident from the interference fringe shift across the front. Figure 3(b) shows fits along two cuts across the front as indicated on the interferogram. Figure 3(c) shows the trajectories of the field across the front, and Fig. 3(d) gives respective amplitudes and phases. The cut A70 is clearly a "gray" front with a smooth phase profile and a considerable imaginary part of the field in the middle of the front. The cut A40, conversely, is very close to an Ising (real) front as the near zero amplitude minimum and the abrupt phase change across the front indicate. The field trajectory lies almost on the real axis.

We found it never quite possible, however, to reconstruct a black front (i.e., the amplitude reaches zero, the imaginary part of the field is zero throughout, and the phase changes by π in step-function manner). This indicates that formula (1) may not precisely describe curved fronts in 2D.

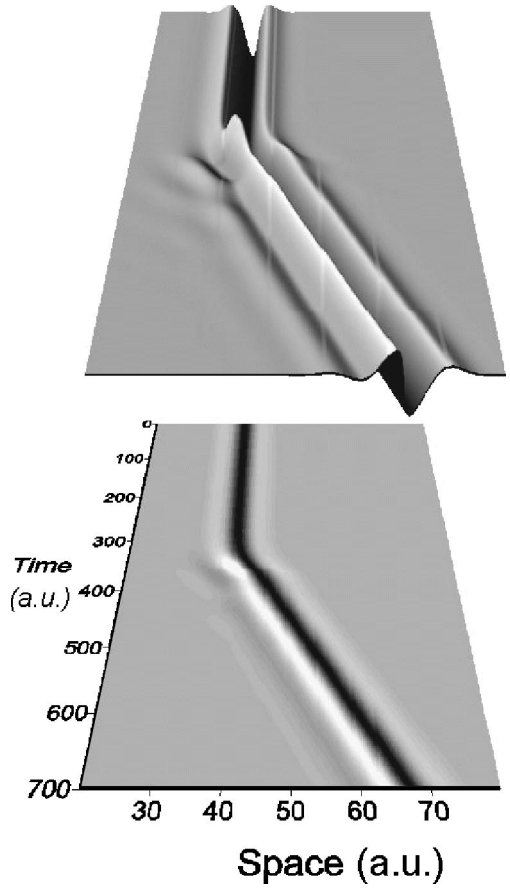

FIG. 9. Ising-Bloch transition in a one-dimensional resonator (detuning=0.1).

The reconstruction of the entire 2D complex field by the Fourier method was therefore employed. Figures 4(a) and 4(b) show an experimental intensity picture and its interferogram, where the reconstructed values of phase and amplitude are displayed in Figs. 4(c) and 4(d). One can see gray front pieces with corresponding smooth changes of phase, marked by arrows, and black front pieces with abrupt phase change.

In the phase picture [Fig. 4(c)], the phase changes by 2π from black to white. There appear to be changes of 2π across the front in certain front pieces. This 2π change, however, is an artifact stemming from the multivaluedness of the inverse trigonometric functions. The true phase change across the front is always $\sim\pi$.

Figure 5 illustrates the different front characteristics by a cut showing a gray front on the left and a black front on the right. One can clearly see that the phase, as expected, changes across both fronts by π, smoothly for the gray front and abruptly for the black front.

Figure 6 shows the field trajectory across the front pieces *b* and *i* [analogously to Fig. 3(c)], illustrating further the complex character of the front *b* and the real character of the front *i* of Fig. 5.

As pointed out previously one would expect to find some relation between grayness, curvature and front velocity. Figure 7(a) shows, as an example, such relation between front grayness and curvature, and velocity and curvature, obtained by analysis of the dynamics of two different fronts recorded

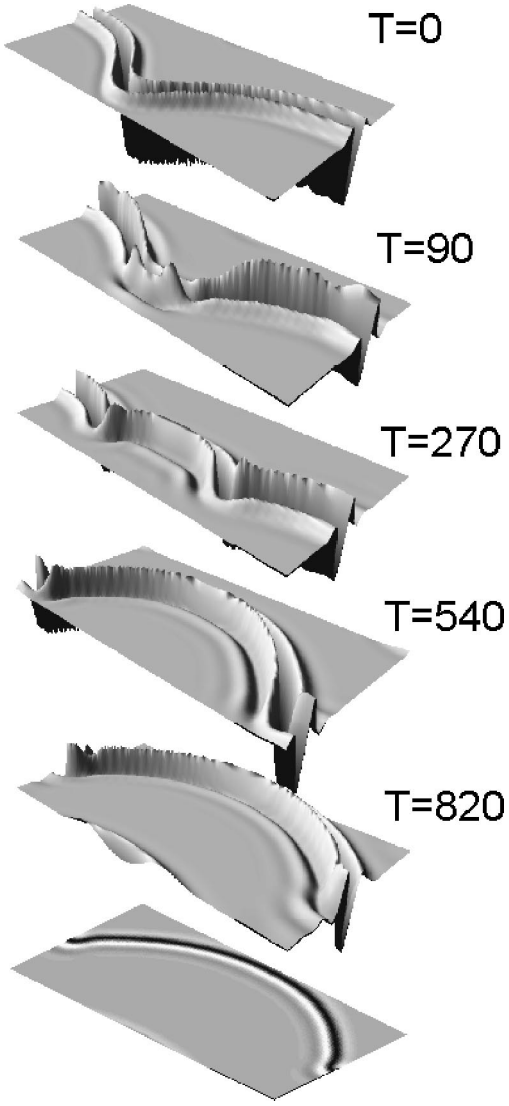

FIG. 10. Ising-Bloch transition and formation of a moving Bloch front in a two-dimensional resonator for small detuning (detuning=0.1, initial condition: a curved Ising front, size of the displayed window: 70×140).

experimentally. One can clearly see that front *i* in the limit of zero curvature (i.e., a straight front) becomes black (Ising type) without any motion. On the other hand, front *b* at zero curvature has finite grayness at finite velocity, which means that a straight gray (Bloch type) front with motion exists. This shows that an Ising-Bloch transition for straight fronts can occur for the experimentally accessible parameters. Figure 7(b) gives, as an example, the front *i* with curved section, straightening in time.

III. MODEL

To explain the existence of complex fronts in 2D degenerate four-wave mixing a model beyond the SHE approximation is needed. We use here a more microscopic description of the photorefractive resonator. Four fields interact in the photorefractive crystal. Two counter propagating beams

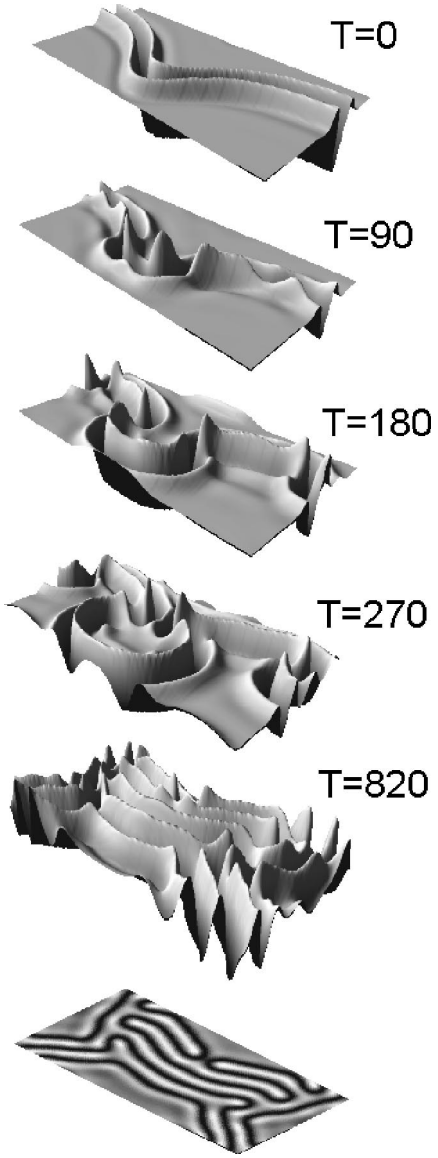

FIG. 11. Ising-Bloch transition and formation of a labyrintic pattern in a two-dimensional resonator for large detuning (detuning=0.2, initial condition: a curved Ising front, size of the displayed window: 50×100).

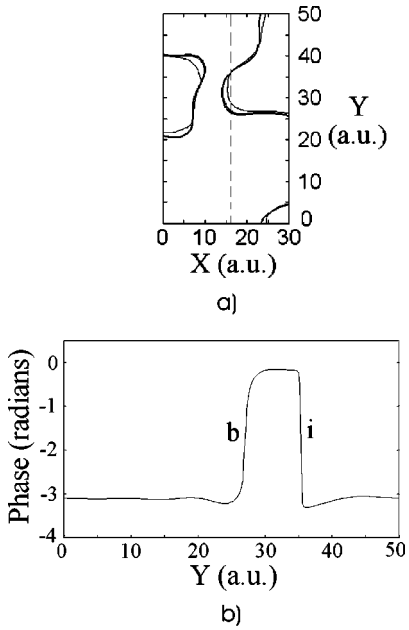

FIG. 12. (a) Phase pattern calculated at detuning=0.1, dotted line shows a cut taken for (b); (b) a cut showing a gray front *b* on the left and a black front *i* on the right side of the picture (compare with Fig. 5).

pump the crystal under an angle of about 40° with respect to the resonator axis. The field in the resonator is driven mainly by two processes. First a cavity field forms an interference pattern with one of the pump beams. As known for photorefractive oscillators the respective carrier grating scatters a part of this pump beam into the cavity, thus amplifying the same cavity field. This so-called beam-fanning or two wave mixing only needs two waves to interact. But the grating can also be read out by the respective counter propagating pump wave. The respective scattered light amplifies the cavity field, which propagates into the opposite direction. Hence, four waves are involved. In the first case a laserlike action is obtained, while the second process causes phase conjugation. Note that in the linear cavity used, forward and backward propagating waves are coupled by the mirrors. They are represented by a single complex field. The whole process can approximately be described by the following set of normalized equations:

$$\left(\frac{\partial^2}{\partial X^2}+\frac{\partial^2}{\partial Y^2}+D+i\right)U(X,Y,T) = i\gamma_p I_p N(X,Y,T)+\gamma_c I_p N(X,Y,T)^*, \tag{2a}$$

$$\frac{\partial}{\partial T}N(X,Y,T)+N(X,Y,T)=U(X,Y,T)[1-N_0(X,Y,T)], \tag{2b}$$

$$\frac{\partial}{\partial T}N_0(X,Y,T)+\frac{1}{T_0}N_0(X,Y,T) = [|U(X,Y,T)|^2+I_p][1-N_0(X,Y,T)], \tag{2c}$$

where U is the optical field in the resonator. The optical response of the cavity (a few nanoseconds) is orders of magnitude faster than that of the material (seconds). Therefore no time derivative is present in Eq. (2a) for the optical field. The optical field is subject to diffraction with respect to the two transverse coordinates X and Y. The respective spatial scale is the inverse angular half width of the resonance of the resonator. Cavity losses are scaled to an imaginary unit. In addition the resonator might be slightly detuned from its resonance by a value D in units of the half width of the resonance. The optical field is driven by pump light scattered from the gratings. Respective terms appear on the right-hand side of Eq. (2a). γ_p and γ_c are the coefficients of the laserlike and of the phase-conjugation process. Because the pump light is not influenced by the process the only dynamical quantity of the scattering is the amplitude N of the respective

grating. Since the induced grating carries a phase imprint N is a complex quantity. In contrast, the total amount of carriers N_0 is real valued. It accounts for the saturation of the crystal and is scaled to the saturation density. Time T is scaled to the lifetime of the grating, which is mainly determined by diffusion and amounts to a few seconds. The lifetime of the generated carriers is again a few orders of magnitude bigger. T_0 marks its relation of the lifetime of the grating.

Since the required data of the photorefractive crystals are not well known, we have to fit the respective constants. In the simulations we used $T_0=100$, $I_p\approx 0.028$, $\gamma_p=53$, and $\gamma_c=108$. In particular, the strength of the nonlinearity and consequently the magnitude of the scaled pump intensity I_p are not well known. However, general trends and phenomena observed in the experiment can be well reproduced. By varying the detuning one can easily change from collapsing localized structures, for small detuning, to stable cavity solitons, for larger detuning, and finally to growing labyrintic pattern as was observed experimentally in Ref. [2]. In the simulations (Fig. 8) we observe both real-valued domain boundaries and complex ones. The complex-valued domain walls are related to curvature, i.e., the larger the curvature is the more gray the front [Fig. 8(b)] is, in agreement with the experimental finding (Fig. 7).

The model introduced above shows an Ising-Bloch transition for the given parameter set and for a scaled pump power of $I_p\approx 0.0085$. If the system can only evolve with respect to one transverse dimension, this transition is clearly visible (see Fig. 9). In 1D the Ising fronts are unstable and any perturbations will lead to the transformation of symmetric stationary Ising front into asymmetric Bloch-type ones which start to move. In 2D the dynamics is much more involved because curvature driven dynamics interacts with the Ising-Bloch transition. Starting from a slightly perturbed symmetric front, symmetry breaking occurs on different parts of the front in uncorrelated ways. Hence, different parts can move into the opposite directions at the same time locally increasing the curvature. Two principal cases can be distinguished.

(1) For small detuning (see Fig. 10) the front is modulationally stable. Hence, its length as well as its curvature are reduced and one direction of motion (driven by Bloch type of a front) prevails. Figure 10 shows the transition at small detuning from the unstable symmetric curved Ising front ($T=0$) to the asymmetric moving Bloch front with gradual reducing of a front curvature by the system itself. Unfortunately, it is hard to observe this case directly experimentally. In the real system a front always encloses a finite domain, which tends to shrink and disappears finally. A Bloch-type motion is always mixed with the curvature driven dynamics. An observation is limited by the finite lifetime of real structures.

(2) For larger detuning (see Fig. 11) the front has lost its stability. It now tries to increase the local curvature and to increase its length. Hence, asymmetries, which are originally introduced by the Ising-Bloch transition, are amplified. Finally the evolution stops because the whole domain is covered by a labyrintic pattern where the minimum distance between dark lines is given by the detuning. Bloch fronts remain asymmetric, but are trapped in the pattern. In the simulation this final pattern tends to move according to the global balance of forces induced by the Ising-Bloch transition. Again it is hard to detect this effect experimentally because only a limited domain is accessible. Hence, interaction with boundaries becomes essential. In fact, in some cases we have observed a global motion of the resulting pattern. However, some misalignment, which also could have induced motion, cannot be ruled out.

Hence, we can only compare the phase and amplitude structure of experimentally and numerically determined fronts. Figure 12(b) shows the phase along a cut marked by the dotted line in Fig. 12(a). One can clearly see the fronts of Bloch and Ising nature with phase change by π across the fronts, as in the experiment (Fig. 5).

IV. RESULTS

We have experimentally observed that besides real-valued fronts as predicted by the approximate SHE model in Ref. [1], there are also complex-valued domain boundaries in the field generated by degenerate four-wave mixing in a $BaTiO_3$ resonator. We have applied a 2D Fourier transform technique and a fitting procedure for reconstructing the complex field and the phase and amplitude structure of the fronts. We find the Fourier transform technique to be more generally applicable and the experiment shows that it works well. The theoretical model given in this paper confirms that the field of the fronts surrounding phase domains can, contrary to the Swift-Hohenberg model, which is valid near the emission threshold, be complex valued.

We have analyzed the relation of front velocity and of grayness on curvature both numerically and experimentally. From this we find experimental evidence for a 2D analog to the 1D Ising-Bloch transition; namely, the existence of straight black stationary fronts and straight gray moving fronts.

ACKNOWLEDGMENTS

Ye.L. acknowledges the support by the A.v. Humboldt foundation. A.E. and J.G. acknowledge financial support from Spanish Ministerio de Ciencia y Tecnologia and European FEDER Funds through Projects Nos. BFM2002-04369-C04-01 and BFM2001-3004.

[1] K. Staliunas and Victor J. Sanchez-Morcillo, Phys. Rev. A **57**, 1454 (1998).
[2] V. B. Taranenko, K. Staliunas, and C. O. Weiss, Phys. Rev. Lett. **81**, 2236 (1998).
[3] P. Coullet, J. Lega, B. Houchmanzadeh, and J. Lajzerowicz, Phys. Rev. Lett. **65**, 1352 (1990).
[4] D. Michaelis, U. Peschel, F. Lederer, D. V. Skryabin, and W. J. Firth, Phys. Rev. E **63**, 066602 (2001).
[5] J. A. Arnaud, Appl. Opt. **8**, 189 (1969).
[6] M. Vaupel and C. O. Weiss, Phys. Rev. A **51**, 4078 (1995).
[7] D. Y. Tang, M. Y. Li, and C. O. Weiss, Phys. Rev. A **44**, 7597 (1991).